A Preshower for the STAR FMS

November 06, 2013

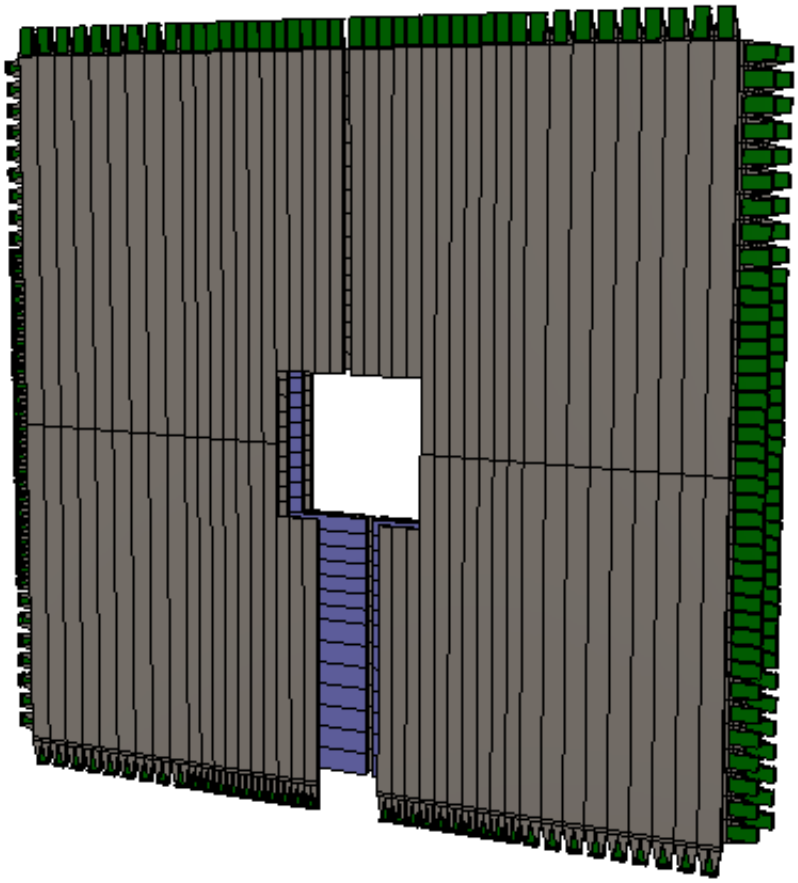

Table of Contents

ABSTRACT

This document describes the physics motivation for a preshower detector in front of the FMS. Further the design, layout, performance, cost and integration of the preshower into STAR are detailed.

1. Physics Motivation for a Preshower Detector in front of the FMS:

1.1. Polarised pp scattering

The RHIC spin physics program seeks to advance our understanding of the spin and flavor structure of the proton in terms of its constituent quarks and gluons, exploiting the unique capability of RHIC to provide access to polarized p+p collisions.
A natural next step in the investigation of nucleon structure is an expansion of our current picture of the nucleon by imaging the proton in both momentum and impact parameter space. At the same time we need to further our understanding of color interactions and how they manifest in different processes. In the new theoretical framework of transverse momentum dependent parton distributions (TMDs) we can obtain an image in the transverse as well as longitudinal momentum space (2+1 dimensions). This has attracted renewed interest, both experimentally and theoretically in transverse single spin asymmetries (SSA) in hadronic processes at high energies, which have a more than 30 years history. First measurements at RHIC have extended the observations from the fixed-target energy range to the collider regime. Polarized nucleon-nucleus collisions may provide further information about the origin of SSA in the forward direction and the saturation phenomena in large nuclei at small x.

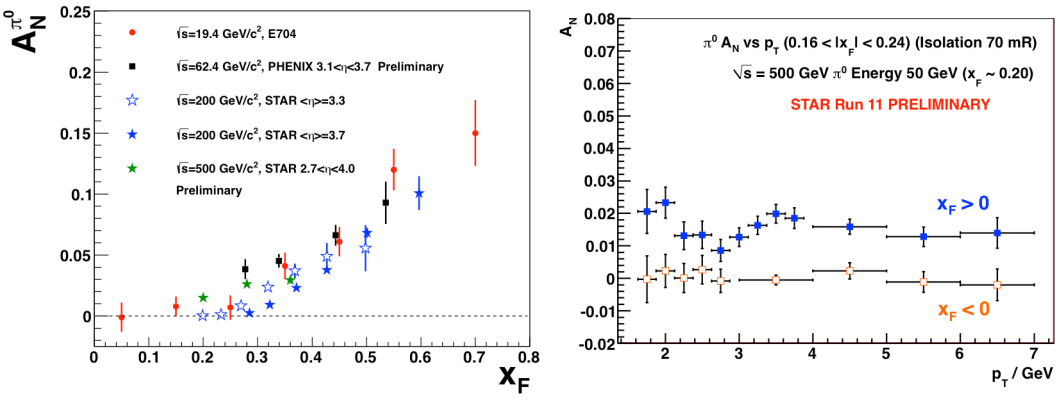

Figure 1-1: Transverse single spin asymmetry measurements for neutral pions at different center-of-mass energies as function of Feynman-x **(left)** and p_T-dependence at $\sqrt{s}$ = 500 GeV **(right)**.

Single spin asymmetries in inclusive hadron production in proton-proton collisions have been measured at RHIC for the highest center-of-mass energies to date, √s = 500 GeV, summarizes the measured asymmetries from different experiments as functions of

Feynman-x ($x_F \sim x_1$-x_2) and transverse momentum. Surprisingly large asymmetries are seen that are nearly independent of $\sqrt{s}$ over a very broad range (see Figure 1-1 (left)). To understand the observed significant SSAs one has to go beyond the conventional collinear parton picture in the hard processes. Two theoretical formalisms have been proposed to generate sizable SSAs in the QCD framework: transverse momentum dependent parton distributions and fragmentation functions, which provide the full transverse momentum information. At RHIC the p_T-scale is sufficiently large to make the collinear quark-gluon-quark correlation formalism, which provides the average transverse information, also an appropriate approach to calculate the spin asymmetries.

STAR has made several important contributions to this program, primarily through study of forward neutral pion production in p+p collisions (see, for example, ref. [1] and Figure 4.2-5). The Run 11 transverse polarized data taken at $\sqrt{s}$ = 500 GeV allow to reveal one more surprising feature the flat dependence of A_N for π^0 as function of p_T, see **Figure 1-1** (right). The high statistics transverse polarized data taken at $\sqrt{s}$ = 200 GeV in Run 12 confirm this behavior. But more importantly the Run 12 data allow studying in more detail the dependence of the π^0 A_N on the event kinematics.
As one can see in Figure 1-2, the asymmetry grows as more isolated the π^0 is, which is in contradiction to what is expected for the Sivers-effect, which should be biggest in jet-like events.

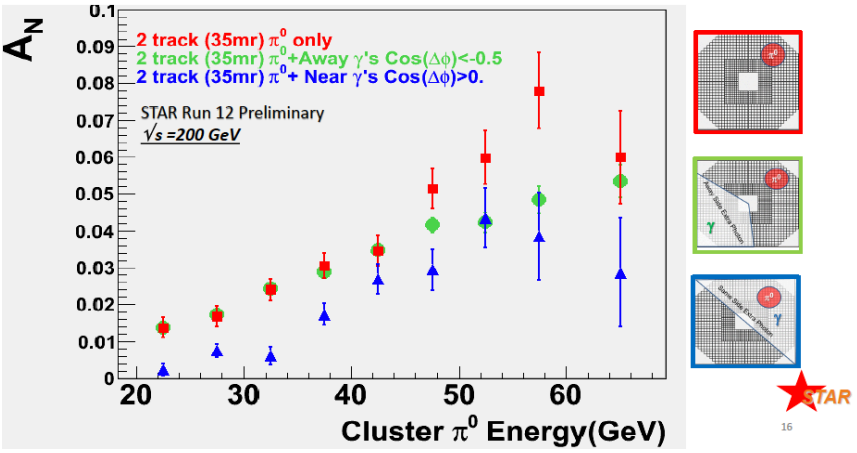

Figure 1-2: A_N for π^0 as a function of the π^0 Energy averaged over the pseudo-rapidity of the π^0 and its p_T with a 35 mrad cone around the π^0. The blue and green points require additional activity outside the π^0 isolation cone, the requirements are indicated in the schematics on the right side. These results make it even more important to extract observables, which are less inclusive.

Table 1-1 identifies observables, which will help to separate the contributions from initial and final state effects underlying the measured A_N, and will give insight to the transverse spin structure of hadrons.

Sivers	Transversity *h(x)* x Collins FF
A_N as function of rapidity and E_T for inclusive jets A_N as function of rapidity and E_γ for direct photons A_N as function of rapidity and p_T for charmed mesons A_N as function of rapidity and p_T for DY and W, Z	Di-hadron correlations within a jet • A_N as function p_T and the invariant mass of the hadron pair (IFF) $A_{UT}^{\sin\Phi} = A_{UT}\sin(\Phi_R - \Phi_S) = \frac{\sigma^{\uparrow} - \sigma^{\downarrow}}{\sigma^{\uparrow} + \sigma^{\downarrow}}\sin(\Phi_R - \Phi_S).$ • A_{UT} as function of the azimuthal dependence of the correlated hadron pair on the spin of the parent quark

Table 1-1: Observables to separate the contributions from initial and final states to the transverse single spin asymmetries.

With its broad acceptance for charged particles in the TPC, STAR is well positioned to carry out the study of di-hadron correlations within a jet, *i.e.*, at relatively small opening angle, where one works with the transverse momentum p_T and the invariant mass of the pair, rather than with individual particle p_T. These Correlations can be described in terms of the product of the transversity *h(x)* and the so-called Interference Fragmentation Function, IFF, which is a chiral-odd quantity. Extracting the IFF in polarized *p*+*p* collisions at high energy is of particular interest as it will constrain *h(x)* at higher values of *x* than competing measurements in semi-inclusive DIS. Recent first results are shown in Figure 1-3.

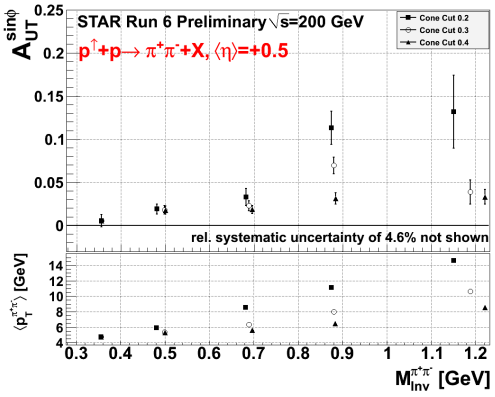

Figure 1-3: (top) Preliminary measurements of the transverse single-spin asymmetry A_{UT}, as defined in the text, as a function of the invariant mass of the unlike-sign di-pion. The choice of cone cut radius is strongly correlated with the average transverse momentum of the pair, as can be seen in the kinematic plot (bottom).

The observable of leading charged pions inside a reconstructed jet is similarly to the IFF case sensitive to the product of transversity *h(x)* and the Collins Fragmentation Function *ΔD(z),* also a chiral odd quantity. Measurements in semi-inclusive deep inelastic and electron-positron scattering have shown *ΔD(z)* to be sizable and increasing with increasing pion momentum fraction *z*. In the pp-case one is looking for correlations between the azimuthal distribution of the pion inside the jet and the spin orientation of the parent proton, see Figure 1-4. To probe the Sivers effect on reconstructs the $\sin(\phi_s)$ modulation of a jet. At mid-rapidity due to the underlying

parton-parton scattering this observable is mainly sensitive to the gluon Sivers function. All observables at midrapidity sensitive to the Sivers function are compatible with zero and such a very small gluon Sivers function. At forward rapidities the dominant process is qg and qq scattering and therefore probes the quark-Sivers function.

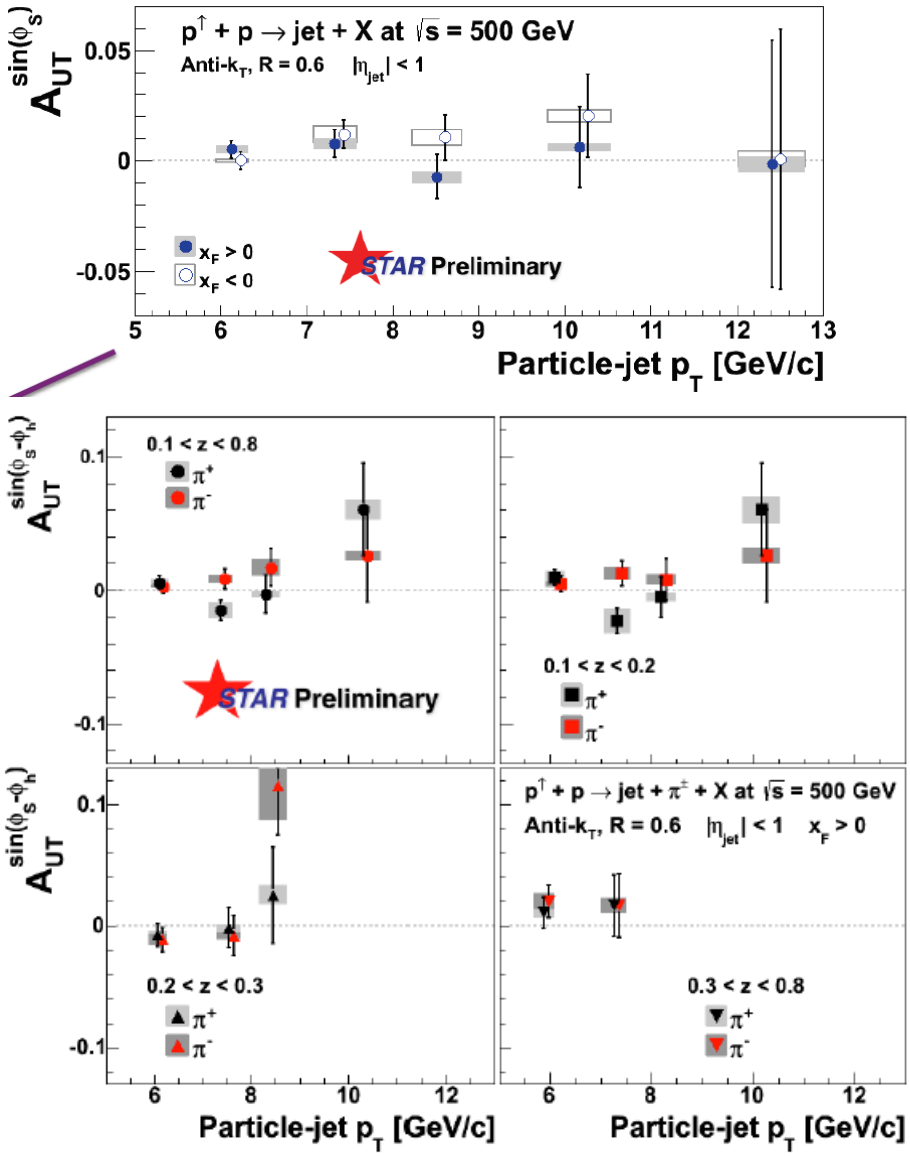

Figure 1-4: Collins (bottom) and Sivers (top) jet-asymmetries as function of the particle-jet p_T from the Run-11 $\sqrt{s}$ = 500 GeV data.

Following the motivation for transverse polarized physics described above a transverse polarized p+p run with an integrated sampled luminosity of 40 pb^{-1} as anticipated for 2015, will allow to answer several open questions, i.e. where does the p_t-dependence of A_N for π^0 turn over from flat and follows the pQCD expected $1/p_T$ behavior?

But most importantly it will give the opportunity to study the underlying sub-processes being responsible for the forward A_N. Having a first measurement of the direct photons A_N with the FMS will be extremely crucial to understand the contribution of the Sivers-mechanism to the forward A_N. For the measurement of the direct photons it will be important to have the pre-shower described below installed in front of the FMS. Direct photons are a rare process. Therefore it is important to suppress background from leptons, hadrons and π^0 as much as possible. As shown by the first simulations the first 2 layers provide a lepton suppression of 96% by keeping 96% of photons, together with the third layer, which provides also 90% rejection of leptons and 85% rejection of hadrons, backgrounds can be suppressed enough allow a measurement of A_N of direct photons. Figure 1-5 shows on the left side theoretical prediction from Ref. [2] using different assumptions or the Sivers function. On the right hand side the projected uncertainty for the prompt photon (= direct–fragmentation photon) A_N. The uncertainty in the fragmentation photon A_N was set to 5%. The 40 pb^{-1} will allow for a measurement, which will be easily able to distinguish between the different model assumptions.

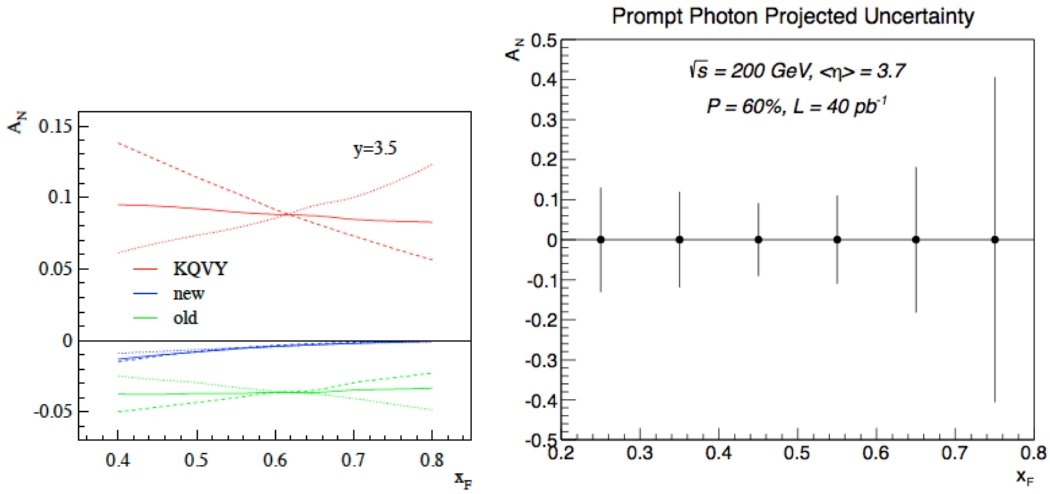

Figure 1-5: (Left plot) Single transverse spin asymmetry for prompt photon production, $p^{\uparrow}+p \rightarrow \gamma + X$, plotted as a function of Feynman x_F at rapidity y = 3.5 and $\sqrt{s}$ = 200 GeV. For each colored curve, the dashed curve is the direct asymmetry A_N^{dir}, the dotted curve is the fragmentation asymmetry A_N^{frag}, and the solid curve is the overall spin asymmetry. The different colors represent different assumptions about the magnitude of the Sivers asymmetry. (Right plot) The projected uncertainty for the prompt photon (=direct–fragmentation photon) A_N. The uncertainty in the fragmentation photon A_N was set to 5%.

1.2. Physics with transversely polarised p+A collisions

1.2.1. Unpolarised observables

Our quest to understand QCD processes in Cold Nuclear Matter (CNM) centers on the following fundamental questions:

- What are the dynamics of partons at very small and very large momentum

fraction (x) in nuclei, and at high gluon-density. What are the nonlinear evolution effects (i.e. saturation)?

- What are the pQCD mechanisms that cause energy loss of partons in CNM, and is this intimately related to transverse momentum broadening?
- What are the detailed hadronization mechanisms and time scales and how are they modified in the nuclear environment?

Various aspects of these questions are being attacked by numerous experiments and facilities around the world. Deep inelastic scattering on nuclei addresses many of these questions with results from HERMES at DESY [3,4], CLAS at JLab [5], and in the future at the JLab 12 GeV upgrade and eventually an Electron-Ion Collider [6]. This program is complemented with hadron-nucleus reactions in fixed target p+A experiments at Fermilab (E772, E886, and soon E906) [7] at the CERN-SPS.

Current measurements at RHIC of the suppression of single hadrons [8,9] and back-to-back di-hadron correlations [10] in d+Au collisions have been interpreted as strong hints that the saturation scale, and the onset of saturation effects are accessible at forward rapidities at RHIC [11]. At this point, though, these interpretations are not unique.

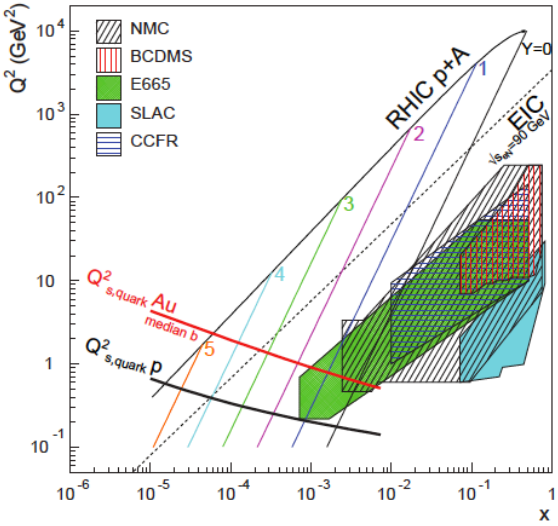

Figure 1.2-1: Kinematic coverage in the x-Q^2 plane for p+A collisions at RHIC, along with previous e+A measurements, the kinematic reach of an electron-ion collider (EIC), and estimates for the saturation scale Qs in Au nuclei and protons. Lines are illustrative of the range in x and Q^2 covered with hadrons at various rapidities.

First, as shown in Figure 1.2-1, for the kinematic reach of RHIC energies the saturation scale is moderate, on the order of a few GeV^2, so measurements sensitive to the saturation scale are by necessity limited to semi-hard processes, and effects due to kinematic limits must be fully addressed. To some level this can be addressed at the LHC, where the larger energies allow for measurements deeper into the saturation regime, especially at forward rapidities.

The higher luminosity in the upcoming 2015 p+A run will also enable to study more luminosity hungry processes, i.e. direct photon, photon – jet, photon - hadron correlations.

Beyond establishing saturation in the RHIC pA/dA data the performance milestone DM8 (2012) asks for measuring the gluon densities at low x in cold nuclei via pA or dA

collisions. The golden channel for this is direct photon production at forward rapidities. As described earlier to measure direct photons with the FMS a preshower detector is essential.

To answer the 3 questions listed above it is important to measure different observables to different final states. By comparing at forward rapidities R_{pA} for hadrons, J/Ψ, and photons sensitivities to pure initial state effects, effects due to energy loss of heavy quarks vs. light quarks as well as saturation effects can be given different emphasis.

The plot below shows the current possibility to extract a J/Ψ-signal from the 2008 pp FMS data. Having a preshower in front of the FMS will reduce the background due to photons significantly. This will make a R_{pA} measurement feasible.

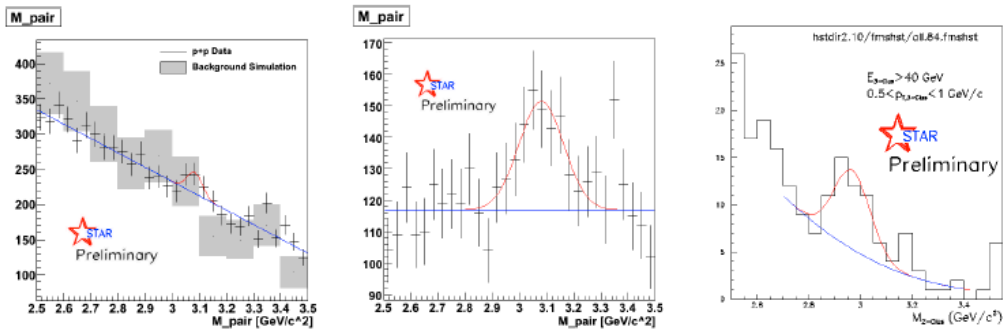

Figure 3: (a) Reconstructed invariant mass at forward rapidity in *p+p* collisions with original cuts for 2-cluster analysis. Errors bars on data points are statistical only. Blue curve shows fitted background. Red curve shows fitted J/ψ signal. Gray bands show simulated background. (b) Reconstructed invariant mass at forward rapidity for 2-cluster analysis with additional cuts on cluster p_T. (c) Reconstructed invariant mass of pair associated with J/ψ in 3-cluster analysis.

A very recent development is that, within well-defined approximations, the saturation scale for gluons can be related to the gauge-invariant Transverse-Momentum-Dependent (TMD) gluon distribution [12] in a nucleon embedded in a nucleus [13], connecting to the saturation scale via a dipole approximation. Within the dipole picture, the saturation momentum has been shown to be equal to the transverse momentum broadening for the Drell-Yan and quarkonia production processes on a nucleus [14]: $Q^2_{sat}(b, E) = \Delta p^2_T(b, E)$, where b is the impact parameter and E is the energy of the parton propagating through the medium. The physical origin of the broadening is the interaction of a propagating parton with the transverse gluonic field in the medium through gluon bremsstrahlung. The probability of gluon radiation is proportional to the gluonic parton density of the medium, and thus p_T broadening is a direct measure of the saturation phenomenon. The value of Δp^2_T has been measured in a small number of experiments where the lab-frame parton energies range from 2 GeV to 270 GeV, see Figure 1-2

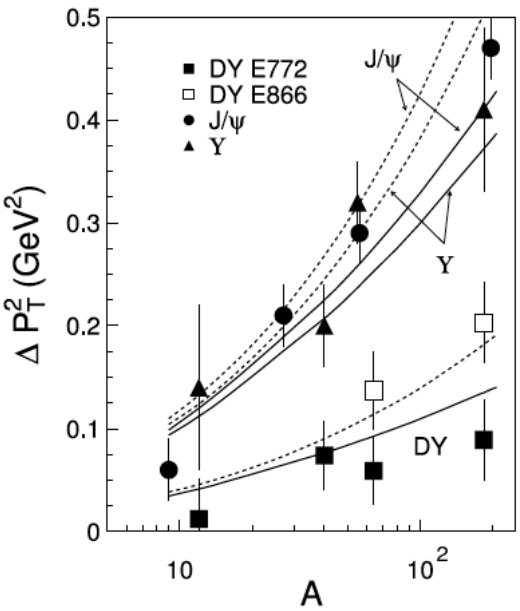

Figure 1.2-2: Broadening in Drell-Yan reactions on different nuclei as measured in the E772 (closed squares) [15] and E866 (open squares) [16] experiments respectively. Broadening for J/Ψ [15, 16] is shown by circles and triangles respectively. The dashed and solid curves correspond to the predictions without and with the corrections for gluon shadowing.

1.2.2. Polarised observables

Single Transverse Spin Asymmetry in Polarized Proton-Nucleus Collisions: As a result of exciting recent theoretical developments, the scattering of a polarized proton on an unpolarized nuclear target appears to have the potential to extend and deepen our understanding of QCD. In the frame where the nucleus is relativistic, its wave function consists of densely packed quarks and gluons, which constantly split and merge with each other. At high enough energies the density of the gluons is so high that the saturation regime is reached, characterized by strong gluon fields and scattering cross sections close to the unitarity bound. The saturated wave function is often referred to as the Color Glass Condensate (CGC) and is reviewed in detail in [17-21].

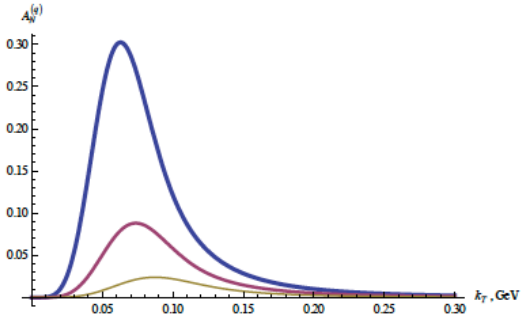

Figure 1.2-3: Quark SSA from Eq. (81) in [22] plotted as a function of k_T for different values of the target radius: R = 1 fm (blue curve), R = 1.4 fm (red curve), and R = 2 fm (gold curve) for $\alpha = 0.7$.

Scattering a polarized probe on this saturated nuclear wave function may provide a unique way of probing the gluon and quark transverse momentum distributions (TMDs). In particular, the single transverse spin asymmetry A_N may provide access to the elusive nuclear Weizsaecker-Williams (WW) gluon distribution function [23,24], which is a solid prediction of the CGC formalism [25,26] but is very difficult to measure experimentally. The nuclear effects on A_N may shed important light on the strong interaction dynamics in nuclear collisions. While the theoretical approaches based on CGC physics predict that hadronic A_N should decrease with increasing size of the nuclear target [27-31] (see Figure 1.2-3), some approaches based on perturbative QCD factorization predict that A_N

would stay approximately the same for all nuclear targets [32]. The asymmetry A_N for prompt photons is also important to measure. The contribution to the photon A_N from the Sivers effect [33] is expected to be non-zero, while the contributions of the Collins effect [34] and of the CGC-specific odderon-mediated contributions [35] to the photon A_N are expected to be suppressed [31,36].
Of course the measurement of the photon A_N requires the preshower in front of the FMS to be present. Clearly experimental data on polarized proton-nucleus collisions is desperately needed in order to distinguish different mechanisms for generating the single spin asymmetry A_N in nuclear and hadronic collisions.

Figure 1.2-4 clearly shows that the requested statistics of 40 pb^{-1} and 300 nb^{-1} for p+p and p+Au, respectively, are sufficient to measure transverse spin observables in pA. The curves represent the theoretical prediction [31] for the suppression of SSA in the nuclear medium. This measurement will not only allow to get a handle on the saturation scale, but will also help to understand the underlying sub-process leading the big forward SSA in transverse polarized p+p. To distinguish further between the different theoretical models predicting a suppression of A_N in p+A, it will be also essential to measure A_N for direct photons. More details about the pre-shower in front of the FMS and its performance as well as the capabilities to measure A_N for direct photons can be found in section **Error! Reference source not found.**.

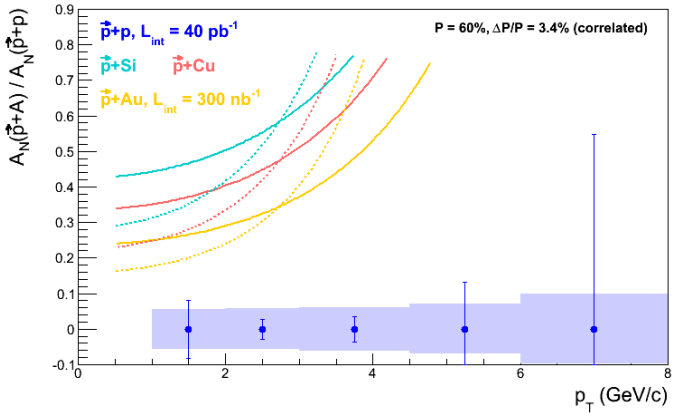

Figure 1.2-4: The projected statistical and systematic uncertainties for the ratio of A_N^{pA}/A_N^{pp} measured for π^0's in the STAR FMS for the requested transverse p+p and p+A running. The colored curves follow Eq. 17 in Ref. [31] assuming Q_s^p = 1 GeV (solid) and Q_s^p = 0.5 GeV (dotted) with $Q_s^A = A^{1/3} Q_s^p$.

2. Preshower Design and Simulation Results

Preshower Design:
We propose to install a preshower detector in front of the FMS, which will help distinguish photons, electrons/positrons and charged hadrons. This detector will be comprised of two layers of perpendicularly arranged scintillator slats (PS1 and PS2), followed by a lead converter and a subsequent third layer of scintillator slats (PS3). PS1 and PS2 will be used to identify neutral particles (photons) from charged particles (hadrons and electrons), while PS3 after the converter will help separating electromagnetic showers (photons and electrons) from charged hadrons.

The preshower detector will be located at a little less than 7 m downstream of the nominal interaction point in STAR (in front of the FMS) and will cover a transverse area of about 2x2 m^2 with a 40x40 cm^2 cutout in the center for the beam pipe. The preshower layers will be divided into quadrants. The detector will be segmented to 80 scintillator slats per layer, and the granularity of the array is going to match that of the FMS loosely. Due to space constrains with beam pipe supports and the west platform floor, bottom quadrants will be slightly shorter and have an opening below the beam pipe. The top two quadrants each contain 21 scintillator-slats, and bottom quadrants contain 19 slats. The inner 12 channels have a width of 4 cm, followed by 9 channels with a width of 5.8 cm. The length of the scintillators is 100 cm, or 80 cm where they touch the inner cutout region. Slats in PS1 will be oriented vertically, while PS2 and PS3 to be oriented horizontally as indicated in **Error! Reference source not found.**

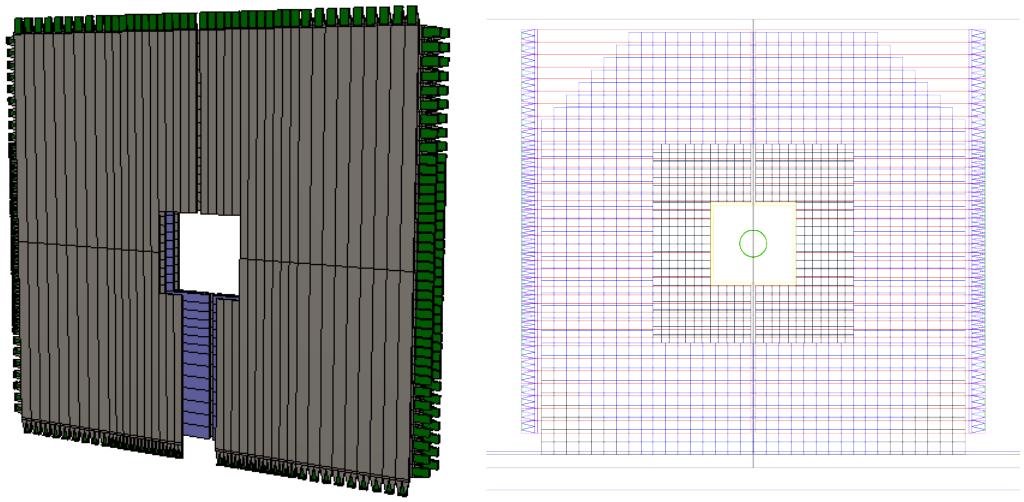

Figure 2-1 Geometry of the layers of a proposed preshower detector in front of the FMS electromagnetic calorimeter in STAR. **Left:** Layered setup of scintillators (grey) with a Pb converter (blue) and SiPM and FEE board (green). **Right:** Matching of granularity of preshower (layer 3, red) with the tower size of the FMS (black and blue).

Signals will be read out by two 3x3mm Hamamatsu 10931-025P MPPC (SiPM), which will be attached to light guides at the end of the scintillator slat as shown in Figure 2-2. The two SiPMs will be connected to a FEE board developed for the forward calorimeter upgrade by Gerard Visser. The FEE board requires a single multi-drop flat cable to bring in LV (5V and -90V) as well as slow control bus, and it will have a Lemo connector for the signal output. The signals will be readout by existing QT boards as a part of STAR trigger system.

There will be 63 (21 x 3 layers) channels for the two top quadrants, and 58 (19 x 3 layer) channels for the two bottom quadrants. Those signals will feed 8 QT boards for readout. Existing FMS QT1-4 crates have 2 empty slots each, which can be utilized for the preshower readout.

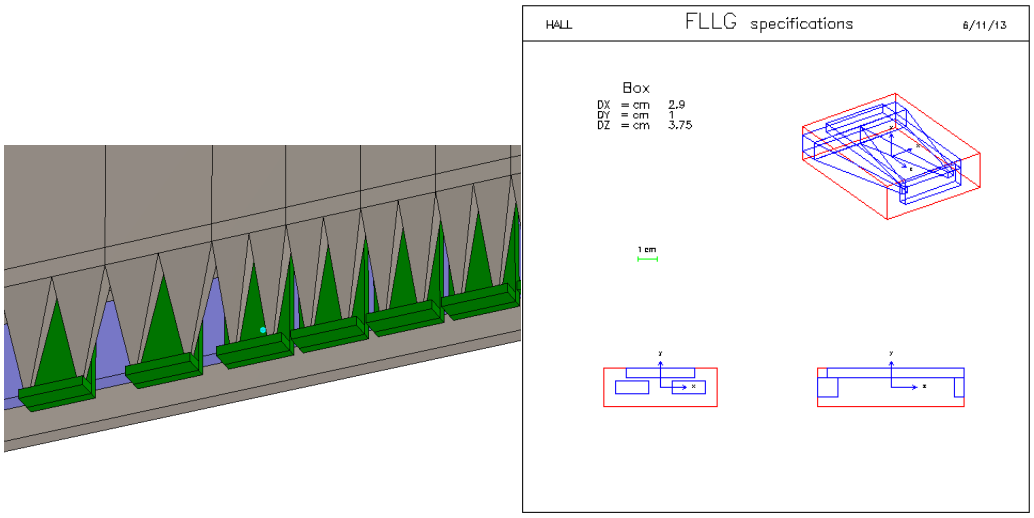

Figure 2-2: To keep taper angle small while making it compact, there will be one light guide with a "two mountain structure" glued at each end of a scintillator slat. A small board with two SiPM will be attached to the end of the light guides. FEE board will be mounted along the light guide for compactness as well as to give mechanical stability.

Some words to the choice of 3x3mm Hamamatsu 10931-025P MPPCs as readout instead of conventional PMTs. At the location of the preshower the stray magnetic field of the STAR solenoid can vary in direction and magnitude very dramatically. Values up to 400 gauss have been measured. This would require massive magnetic shielding of the PMTs, which would apart from the cost make each quadrant significantly more heavy and difficult to handle. There was an option like for the FMS to obtain PMTs from FermiLab for free, but like for the FMS the bases would ahave to be modified as they would be wider as the individual width of the SC-slats. With all the improvements and experience by other groups it seems to be low risk to move to SiPMs for the readout, especially as the project can benefit from the already designed readout cards.

Simulations:

Energy loss in the scintillators is primarily by ionization and the particles from the high energy proton-proton collisions are almost exclusively in the range where they are considered minimum ionizing particles. Electrically charged particles lose energy by dE/dx, so the deposited energy in the scintillator is proportional to the thickness of the active element. Photons on the other hand do not lose any energy by simple ionization. Layers 1 and 2 of the preshower can then be combined to identify electromagnetic clusters in the FMS that originate from high energetic photons.

Initial simulation studies of the detector response have been carried out with different settings of the scintillator thickness as well as the preshower layer. Assuming a certain required rigidity of the detector setup, we have varied the thicknesses of the layers between $10 < \Delta z < 20\ m$m each. We looked at single particles that were thrown in flat energy (10 < E < 40 GeV) at a well defined location in the prehower. Studies included photons, electrons, pions, and muons.

While the measured (deposited) energy of charged particles is directly proportional to the thickness of the active element, the identification (or rejection) of photons is only very weakly dependent on this parameter. This is due to the increased probability of the photon to induce an electromagnetic shower the more material is traversed. With a proper adjustment of the threshold for charged particle identification (in the few MeV range), the two effects compensate each other. Single photonic clusters in the FMS can be identified at a level of more than 96% when matched with the first two preshower layers. Minimum ionizing particles are rejected at about the same level. This simulation does not include effects from the readout and electronics, but the additional dilution is expected to be small.

Layer 3 of the preshower is intended to separate hadronic contributions in the electromagnetic clusters. Both photons and electrons are likely to initiate an electromagnetic shower in the Pb-preshower layer whereas hadrons will only do so after a hadronic collision. In the following, the ionization in the scintillator will be largely amplified for electrons and photons depending on the thickness of the lead layer. The rejection level for hadrons is better than 85% with an electron identification efficiency of more than 90%. Again, this result is independent of the scintillator and the Pb preshower thickness and it is consistent with the relation between radiation length and nuclear interaction length in lead, see Figure 2-3.

As the rejection curve flattens out at high values, there seems to be slight preference towards thicker scintillators in combination with more preshower material (≈ 15 mm) depending on the threshold energy for hadrons and the stability of the readout. The absorber material will also affect the energy response in the FMS, though, which has to be taken into account. Part of this will lead to a dilution that cannot be corrected for in the end.

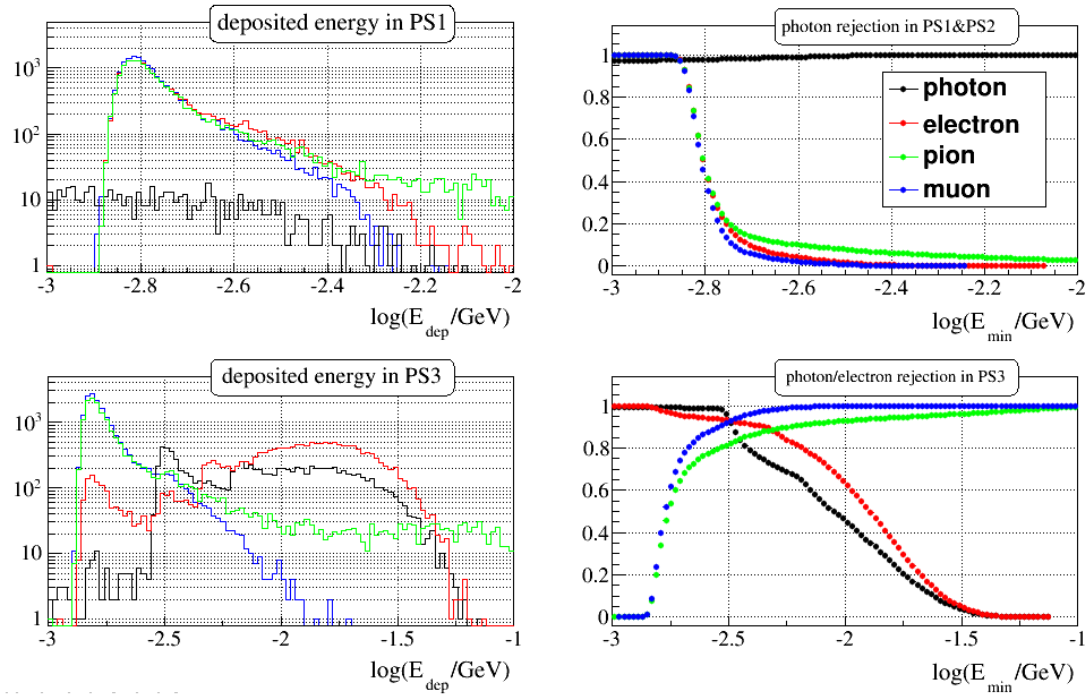

Figure 2-3: Simulation studies of the preshower detector response for single particles with energies of 10 to 40 GeV and scintillator (thickness 10 mm) and lead layer (thickness 6 mm). **Left:** Deposited energy in scintillator layers PS1 and PS3. Layer PS2 shows a response similar to PS1. **Right:** Photon and electron identification capabilities as function of minimum deposited energy. Note the different logarithmic energy scales for the different preshower layers (top and bottom).

The main background for direct photons comes from photonic decays and other mesons produced in fragmentation from hard partonic scattering processes (QCD $2 \rightarrow 2$). This type of background can be studied in event generator simulations based on PYTHIA (version 6.4.21) and a set of parton distribution functions from a global fit to world data (CTEQ6).

Especially in the forward direction, the simulation needs careful comparison with existing data (e.g. cross section of pion production in proton-proton collisions at RHIC) and NLO pQCD calculations to show the validity of the approach. Depending on the kinematic range and settings of the simulation, a few 10 to 100 million events have to be generated. In particular the transverse component of the momentum in the hard scattering $\hat{p}_{\perp}$ has been shown to be critical in order to obtain sensible results. Depending on the threshold value for the event generation, it can lead to an unphysical dominance of the higher-order process cross section over the leading order. This is especially important in forward kinematics, where the average transverse momentum of a final state particle is small compared to that of a midrapidity particle.

Although PYTHIA tends to overestimate pion production at larger rapidities, overall there is a fair agreement with existing data at 200 GeV and the NLO pQCD calculations at 200 and 500 GeV. For initial background studies with a conservative assumption, the cross section of direct photon production is about two orders of magnitude smaller than the hard QCD $2 \rightarrow 2$ processes.

Since the preshower design is based on layers with horizontal and vertical scintillator slats, it is vital to show that the matching of hits with clusters in the FMS will work with track multiplicities in proton-proton collisions at 200 GeV (ideally, also at higher energies up to 500 GeV). Identification of leptons in the third scintillator layer can improve direct photon measurements, but will primarily help with heavy flavor measurements, which include single electrons and muons or di-lepton decays.

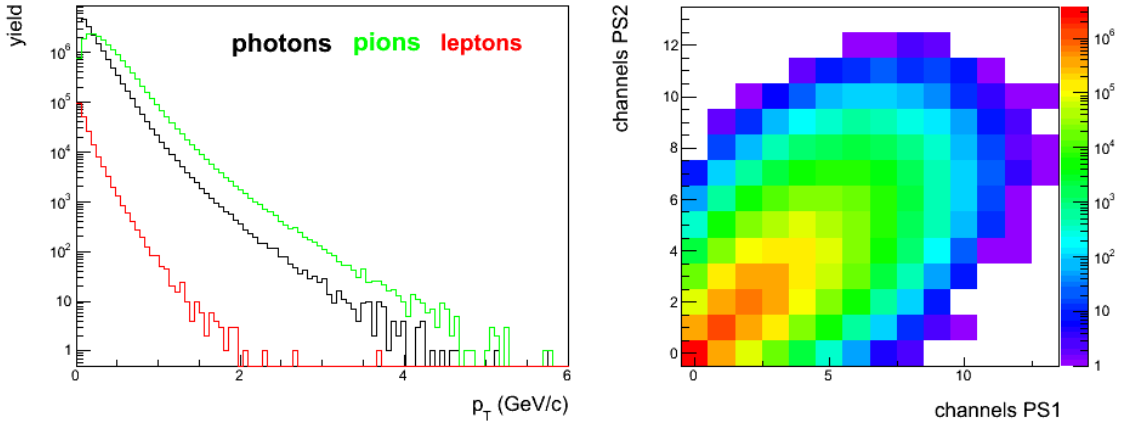

Figure 2-4: Unbiased PYTHIA event generator studies for proton-proton collisions at $\sqrt{s} = 200$ GeV. **Left:** Transverse momentum distributions for photons, pions, and leptons in the acceptance of the FMS calorimeter ($2.4 < \eta < 4.0$) based on 10M simulated events. **Right:** Number of channels with at least one charged hit in one quarter of preshower layers PS1 and PS2. For matching with clusters in the FMS ambiguities may not be resolved for two or more hits in both layers.

Since the preshower can in principle be divided into four independent quarters, it is sufficient to study the track multiplicities of charged particles in one of these quarters. Figure 2-4 on the left shows the transverse momentum distributions for photons, charged pions and leptons that fall within the acceptance of the FMS generated from PYTHIA at $\sqrt{s} = 200$ GeV. We have generated a total of 10M events for this unbiased study. The right plot contains the expected channel multiplicities based on charged tracks only in one quarter of preshower layers PS1 and PS2 (note the logarithmic z-scale). The distribution clearly peaks at single hits in both layers, but it is fairly wide and spreads out to larger values. Any event with hits in two or more channels per layer creates ambiguities that need to be resolved in combination with the third layer and the clusters in the FMS.

The detector response should enable a clear distinction of single and multiple hits in separate channels, but this has to be studied with fast smearing simulations that include photons and early development of electromagnetic showers. Also more detailed simulations are needed with a full description of the detector and modeling of the detector response (ideally with the full offline clustering algorithm) in the FMS for a proper matching with the hits in the preshower layers.

3. Integration into the STAR detector

At meetings with John Scheblein, the STAR operations group and Stephen Trentalange the design criteria for the FMS preshower to integrate it in to the STAR detector have been defined.
The following important points have been identified.

1. Light weight and compact design
2. Easy movable and maintainable
3. Due to space constrains with beam pipe supports and the west platform floor, SC slats in the bottom quadrants have to be slightly shorter.
4. No interference with the FMS

These criteria let to the design shown in chapter 2. Each preshower layer is split in 4 quadrants with the scintillator paddles covering the 40 cm x 40 cm cutout being 80cm long instead of 100 cm.
John Scheblein is currently working on the details of the Preshower holding structure. It will still take a couple of weeks due to more time pressing projects a full design of the holding structure will be available.

4. Cost, Schedule and Manpower

The costs presented below are either based on actual quotes obtained in the last weeks or on costs for equipment bought in 2013 or engineering estimates. Based on this the total cost of the preshower amounts to **$142555.84**

Scintillator: **Total: $53290.00**

Quote from Saint-Gobain Crystals October 31st 2013

60 BC408 80cm x 4cm x 1cm $186.00	$11160.00
84 BC408 100cm x 4cm x 1cm $188.00	$15792.00
108 BC408 100cm x 5.8cm x 1cm $201.00	$21708.00
10% spare for each type	$4630.00

SiPMs; **Total: $20000.00**

http://www.hamamatsu.com/jp/en/product/category/3100/4004/4113/S10931-025P/index.html
Price is based on a quote from November 2013
500 Hamamatsu 10931-025P $40/piece

Light guides: **Total: $9324.00**

250 LG $37/piece
http://www.emachineshop.com gave a price of $37.00 per piece (machining & material) for the LGs needed for the pixilation of the E864-HCAL as the FMS-Preshower LGs are neither more complicated nor much bigger we assume for the moment same price. We also investigate to make the LGs in the group of W. Brooks in Chile, as this group machined all the LGs for the GLUEX barrel calorimeter. For this option we would have to ship the LG material to Chile and they would machine the LGs.

SiPM Frontend Cards: **Total: $22000.00**

250+20%spare SiPM Frontend cards $72.5/piece

The design of these cards follows completely the design for the STAR forward upgrade HCal frontend card by Gerard Visser.

Cables: **Total: $8731.84**

256 RG-58 with the Postironic connectors $7731.84

1. 256 cables x 40ft = 10240ft x $0.15/ft. = $1536
2. 256 positronix contacts x $3.21/contact = $821.76
3. 256 lemo connectors x $11.50/connector = $2944
4. 32 positronix 8 position shells x $1.94/shell = $62.08
5. Labor per bundle = $74 x 32 bundles = $2368

there is the possibility, which needs to be more carefully investigated to reuse RG-58 with the Postironic connectors from IP-2

the cables for the LV for the SiPMs and the Preshower FEE card as well as for the HV and temperature regulating/monitoring of the system are all based on simple twisted pair. We assume an additional cost of $1000.00

LV powersupplies: **Total: $3000.00**

1 Agilente 6614C for SiPM LV $2500.00

http://www.transcat.com/Catalog/productdetail.aspx?itemnum=35003EC&RCF=1&gclid=CIvPjJCszroCFYqi4AodpigAfg

1 simple 90-100VDC power supply to feed the HV regulator on the FEE board $500

Interface Hardware: **Total: $2220.00**

1 linux PC rack mounted	$1500.00
24 link USB $30/piece	$720.00

the linux PC rack mounted can come happily be one sorted out by RACF or the STAR DAQ, in this case the cost drops to $0.00

Lead Sheet: **Total: $4000.00**

4 pieces 1 m x 1 m x 0.6cm lead sheet in a packing to keep it in shape $1000/piece

Conservative estimate by Dr. W. Christie and John Scheblein

Holding Structure and other infrastructure items: **Total: $20000.00**

Conservative estimate by Dr. W. Christie and John Scheblein

Readout Electronics:

As readout electronics the standard STAR QT-boards will be used. Enough channels should be available from the purchase of STAR QT-boards for the A_NDY experiment at IP-2, which is terminated.

Manpower:

For the fabrication of the holding frame and installation in STAR support from the

STAR operations group is required.
The manpower involved/available for the preshower is
BNL: Akio Ogawa, Oleg Eyser and E.C. Aschenauer and possibly a fraction of a postdoc
Indiana: A. Vossen, Will Jacobs, Gerard Visser and Scott Wissink,
ITEP: Igor Alekseev, Dmitry Svirida and most possibly a student, i.e. Dmitry Kalinkin

Schedule and Milestones:

A rough schedule and milestones of the project include:

1. a system test till end of March. This would comprise a test of the several SC slats with the Hamamatsu 10931-025P and the STAR HCal FEE-card first with cosmics and end of February 2014 at the calorimeter test beam at FermiLab.
2. March 2014 analysis of the test beam data and a test of one or 2 SC slats in STAR to investigate neutron damage of SiPMs. This test would not need any readout. Just having slats at the FMS location and measuring before and after one week of beam the gain of the SiPMs
3. By end of April 2014 all final equipment should be ordered.
4. The detector should be fully assembled by September 2014
5. September 2014 till installation cosmic test of the full preshower
6. The Preshower can only be installed in STAR after the FMS is fully assembled and tested.

In parallel to 1 to 7 the analysis software of the preshower is developed and integrated in the STAR software framework. Of course also monitoring plots and other important information for the shift crew will be developed.
It will be absolutely required that the FMS offline analysis software is integrated into the STAR software framework, without this it will be impossible to do the physics described in chapter 1.

5. Benefit to other Projects:

Having the FMS preshower readout based on SiPMs has benefits to at least two other planned projects in STAR.

1. it will test the SiPM readout board combination invisioned for the STAR forward upgrade calorimeter in a long-term in situ test
2. There are plans to upgrade the BBCs for the BES. Using a SiPM readout as for the FMS preshower will avoid several currently cumbersome issues with the BBCs.
    a. The long LG fibers
    b. The sensitivity of the currently used PMTs to the magnetic field
    c. The design will become much more compact and easier to handle

6. Addendum

Here are the quotes or engineering estimates as received.

SAINT-GOBAIN
CRYSTALS

FORMAL OFFER

OFFER DATE: Thursday, October 31, 2013

TO: Akio Ogawa
Brookhaven National Laboratory
P.O. Box 5000
Upton NY, 11973
USA

FAX NO: +1 (631) 3445815

PHONE: + (631) 344-5293

OFFER NUMBER: QUO-36364-CD0YY6
OFFER REVISION: 0
PAYMENT TERMS: Net 30 Days
SHIPPING TERMS: FOB Origin
CUSTOMER REF #: NA

Please refer to top offer number when placing an order.

In response to your request, we are pleased to offer the following:

Customer. Notes:	

ITEM	QTY	DESCRIPTION	UNIT PRICE USD	TOTAL PRICE USD
1	60	BC408 80cm x 4cm x 1cm DM Estimated Lead Time: 6 weeks ARO	$186.00	$11,160.00
2	84	BC408 100cm x 4cm x 1cm, DM Estimated Lead Time: 6 weeks ARO	$188.00	$15,792.00

Saint-Gobain Crystals
17900 Great Lakes Parkway Hiram OH, 44234 +1 (440) 834-5696 Fax: +1 (440) 834-7680
Saint-Gobain Ceramics & Plastics, Inc.

SAINT-GOBAIN
CRYSTALS

ITEM	QTY	DESCRIPTION	UNIT PRICE USD	TOTAL PRICE USD
3	108	BC408 100cm x 5.8cm x 1cm, DM Estimated Lead Time: 6 weeks ARO	$201.00	$21,708.00
Lead times are based on our current workloads. A firm delivery date will be provided at the time of order.			**Total**	**$48,660.00**

NOTE: The prices quoted herein are valid for: 60 days

Country of Origin: USA

Note: Saint-Gobain Crystals products are of a highly complex nature. Our commitment under any product sale based on this offer or any further correspondence in this regard shall therefore be limited to the delivery of products complying with the functional specifications expressly mentioned in this Formal Offer and/or contained in written documents (e.g. Technical Instructions) provided by us. Any other functional specification not expressly mentioned in these documents can not be warranted, even if inherent and measured in samples provided by us.

By: _____

Amy Snyder,
Inside Sales Coordinator
Tel: +1 (440) 834-5696
Email: amy.snyder@saint-gobain.com

Any sale made pursuant to this offer will be governed by Saint-Gobain Crystals standard terms and conditions of sale. Your acceptance of this offer is conditioned upon written verification to the satisfaction of Saint-Gobain Crystals of your credit worthiness.

CC:

Cost estimates (materials & vendor services) for FMS PS version of SiPM FEE board
This is 2-SiPM summed, 2 ch temp compensated voltage regulator, board about 35 x 70 mm

G. Visser, IU
11/5/13

Assembly qty 300 (3*4*21 + spares)
Total cost $ 22,151

Item	Qty/bd	Assy Excess	Qty needed	Mult	Qty buy	Cost ea.	Line cost	BOE/notes
signal conn (EPK.00.250.NTN)	1	1	300	1	300	$ 12.37	$ 3,711	online pricing (Digikey)
pwr/control conn (N3314-5202RB)	1	1	300	1	300	$ 1.69	$ 507	online pricing (Digikey)
DAC (AD5622)	3	1.05	945	1	945	$ 1.67	$ 1,580	online pricing (Digikey)
voltage reference (ADR433ARMZ)	1	1.05	315	1	315	$ 4.24	$ 1,335	online pricing (Digikey)
DS2413	1	1.05	315	1	315	$ 1.24	$ 389	online pricing (Digikey)
regulator opamp (LTC6081)	1	1.05	315	1	315	$ 2.18	$ 687	online pricing (Digikey)
regulator feedback R	2	1.05	630	1000	1000	$ 0.04	$ 40	online pricing (Digikey)
regulator transistors	4	1.05	1260	1	1260	$ 0.16	$ 202	aggregate estimate
bias bypass cap	2	1.05	630	1	630	$ 0.36	$ 224	online pricing (Digikey)
5V regulator (LT1761)	1	1.05	315	1	315	$ 1.92	$ 605	online pricing (Digikey)
tantalum cap (TPSB476K010R0250)	2	1.05	630	1	630	$ 0.51	$ 319	online pricing (Digikey)
preamp transistor (BFR92AW)	2	1.05	630	1	630	$ 0.17	$ 109	online pricing (Digikey)
preamp opamp (OPA836)	3	1.05	945	250	1000	$ 1.25	$ 1,252	online pricing (Digikey)
various R	48	1.1	15840	1	15840	$ 0.03	$ 396	aggregate estimate
various C	17	1.1	5610	1	5610	$ 0.07	$ 373	aggregate estimate
printed circuit board	1	1	300	1	300	$ 11.74	$ 3,522	online quote (Sierra Circuits)
contract assembly	1	1	300	1	300	$ 23.00	$ 6,900	online rough estimate (Sierra)

References:

[1] B. I. Abelev *et al.* (STAR Collaboration), Phys. Rev. Lett. **101**, 222001 (2008), arXiv: 0801.2990 [hep-ex].
[2] L. Gamberg and Z.-B. Kang, Phys.Lett. B718 (2012) 181-188
[3] HERMES Collaboration, A. Airapetian et al., Phys. Lett. B684:114–118, 2010. arXiv:0906.2478
[4] HERMES Collaboration, A. Airapetian et al., Phys. Lett., B577:37–46, 2003. arXiv:hep-ex/0307023,
[5] W. Brooks, Physics with nuclei at an Electron Ion Collider. 2010. arXiv:1008.0131.
[6] W. Brooks and H. Hakobyan, Nucl. Phys, A830:361c–368c, 2009. arXiv: 0907.4606
[7] E866 Collaboration, M. Vasilev et al., Phys. Rev. Lett., 83:2304–2307, 1999. arXiv:hep-ex/9906010
[8] BRAHMS Collaboration, I. Arsene et al., Phys.Rev.Lett. 93, 242303 (2004), nucl-ex/0403005.
[9] STAR Collaboration, J. Adams et al., Phys.Rev.Lett. 97, 152302 (2006), nucl-ex/0602011.
[10] PHENIX Collaboration, A. Adare et al., Phys.Rev.Lett. 107, 172301 (2011), 1105.5112.
[11] J. L. Albacete and C. Marquet, Phys.Rev.Lett. 105, 162301 (2010), 1005.4065.

[12] Z. Liang, X. Wang, and J. Zhou, Phys. Rev., D77:125010, 2008, arXiv:0801.0434.
[13] B. Kopeliovich, I. Potashnikova, and Ivan Schmidt, Phys. Rev., C81:035204, 2010. arXiv:1001.4281,
[14] J. Peng, P. McGaughey, and J. Moss, arXiv:hep-ph/9905447.
[15] **E866 Collaboration**, M. Vasilev et al. Phys. Rev. Lett., 83 2304, 1999, arXiv:hep-ex/9906010.
[16] D. Alde et al. Phys. Rev. Lett., 66:2285–2288, 1991.
[17] H. Weigert, Prog. Part. Nucl. Phys. **55** (2005) 461.
[18] E. Iancu and R. Venugopalan, hep-ph/0303204.
[19] F. Gelis, E. Iancu, J. Jalilian-Marian, and R. Venugopalan, Ann. Rev. Nucl. Part. Sci. 60 (2010) 463.
[20] Y. V. Kovchegov and E. Levin, Quantum Chromodynamics at High Energy. Cambridge University Press, 2012.
[21] J. Jalilian-Marian and Y. V. Kovchegov, Prog. Part. Nucl. Phys. 56 (2006) 104.
[22] Y. V. Kovchegov and M. D. Sievert, Phys. Rev. D **86** (2012) 034028.
[23] A. Metz and J. Zhou, Phys. Rev. D **84** (2011) 051503.
[24] F. Dominguez, J.-W. Qiu, B.-W. Xiao, and F. Yuan, Phys.Rev. D **85** (2012) 045003; J. Jalilian-Marian, A. Kovner, L. D. McLerran, and H. Weigert, Phys. Rev. D **55** (1997) 5414.
[25] Y. V. Kovchegov and A. H. Mueller, Nucl. Phys. **B529** (1998) 451.
[26] F. Dominguez, C. Marquet, B.-W. Xiao, and F. Yuan, Phys. Rev. D **83** (2011) 105005.
[27] D. Boer, A. Dumitru, and A. Hayashigaki, Phys. Rev. D **74** (2006) 074018.
[28] D. Boer and A. Dumitru, Phys. Lett. **B556** (2003) 33.
[29] D. Boer, A. Utermann, and E. Wessels, Phys. Lett. **B671** (2009) 91.
[30] Z.-B. Kang and F. Yuan, Phys. Rev. D **84** (2011) 034019.
[31] Y. V. Kovchegov and M. D. Sievert, Phys. Rev. D **86** (2012) 034028.
[32] J.-W. Qiu, talk at the workshop on "Forward Physics at RHIC", RIKEN BNL Research Center, BNL, 2012.
[33] D. W. Sivers, Phys. Rev. D **41** (1990) 83.
[34] J. C. Collins, Phys. Lett. **B536** (2002) 43.
[35] M. Walker *et al*., arXiv:1107.0917.
[36] L. Gamberg and Z.-B. Kang, arXiv:1208.1962.